Composites: Part B 43 (2012) 3198–3207

Contents lists available at SciVerse ScienceDirect

Composites: Part B

journal homepage: www.elsevier.com/locate/compositesb

Neural network modelling for shear strength of concrete members reinforced with FRP bars

Rizwan Bashir, Ashraf Ashour *

School of Engineering, Design and Technology, University of Bradford, Bradford BD7 1DP, UK

ARTICLE INFO

Article history:
Received 3 November 2011
Received in revised form 6 March 2012
Accepted 10 April 2012
Available online 21 April 2012

Keywords:
A. Fibres
B. Strength
C. Computational modelling
C. Statistical properties/methods

ABSTRACT

This paper investigates the feasibility of using artificial neural networks (NNs) to predict the shear capacity of concrete members reinforced longitudinally with fibre reinforced polymer (FRP) bars, and without any shear reinforcement. An experimental database of 138 test specimens failed in shear is created and used to train and test NNs as well as to assess the accuracy of three existing shear design methods. The created NN predicted to a high level of accuracy the shear capacity of FRP reinforced concrete members.

Garson index was employed to identify the relative importance of the influencing parameters on the shear capacity based on the trained NNs weightings. A parametric analysis was also conducted using the trained NN to establish the trend of the main influencing variables on the shear capacity. Many of the assumptions made by the shear design methods are predicted by the NN developed; however, few are inconsistent with the NN predictions.

1. Introduction

Reinforcing steel in concrete structures is initially protected against corrosion by the alkalinity of concrete, usually resulting in serviceable and durable construction. However for many structures subjected to aggressive environments, such as bridges, marine structures, and parking garages exposed to de-icing salts, combinations of chlorides, moisture and temperature reduce the concrete alkalinity causing reinforcing steel corrosion and ultimately loss of serviceability. Over the last couple of decades, fibre reinforced polymers (FRPs) have become alternatives to conventional steel reinforcement for concrete structures owing to their non-corrosive and non-magnetic properties [1], making them ideal for severe environments and situations where magnetic transparency is required.

Concrete members reinforced longitudinally with FRP bars develop wider and deeper cracks than those reinforced with steel due mainly to the relatively low elastic modulus of FRPs [13,32,35,38,39]. Wider cracks decrease the shear resistance contributions from aggregate interlock and residual tensile stresses, whereas deeper cracks reduce the shear resistance contribution from the un-cracked concrete in compression [14]. Additionally, owing to the relatively wider cracks and small transverse strength of FRP bars, dowel action contribution to shear resistance can be very small compared with that of steel reinforcement [14]. Hence, the overall shear resistance of concrete members reinforced with longitudinal FRP bars is lower than that of concrete members reinforced with steel reinforcement. Over the last couple of decades, several design guidelines and codes [1,5–7,13,21,22,32,33,39] have been published to address FRP bars as longitudinal reinforcement in concrete members. However, the lack of a universally agreed model for shear means that many practice guidelines and codes are still relying upon empirical equations to predict the shear resistance of FRP reinforced concrete members.

The last few decades have witnessed the growth of artificial neural networks (NNs) applied to different structural engineering problems [17,29,30,40]. NNs are computational tools that have the ability to learn by examples of past data, generalise and thus make predictions for previously unseen input data [30]. Due to their unique characteristics, NNs can be used to solve problems which are complicated, problems that cannot be handled by analytical methods and even problems whose underlying numerical and physical models may not be well-known. In this respect, NNs may be suitable for predicting the shear resistance of concrete members longitudinally reinforced with FRP bars.

2. Currently available shear design guidelines

Several codes and design guidelines addressing FRP bars as primary reinforcement for structural concrete have been recently published worldwide [1,5–7,13,21,22,32,33,39]. Most of these design provisions follow the traditional approach of $V_c + V_f$ for shear design, where V_c is the concrete contribution and V_f is the FRP stirrup contribution. Nevertheless, the concrete contribution V_c is different in the manner that it has been calculated in these guidelines. Most of the shear design provisions in these guides are based on

* Corresponding author.
E-mail address: afashour@bradford.ac.uk (A. Ashour).

1359-8368/$ - see front matter © 2012 Elsevier Ltd. All rights reserved.
http://dx.doi.org/10.1016/j.compositesb.2012.04.011

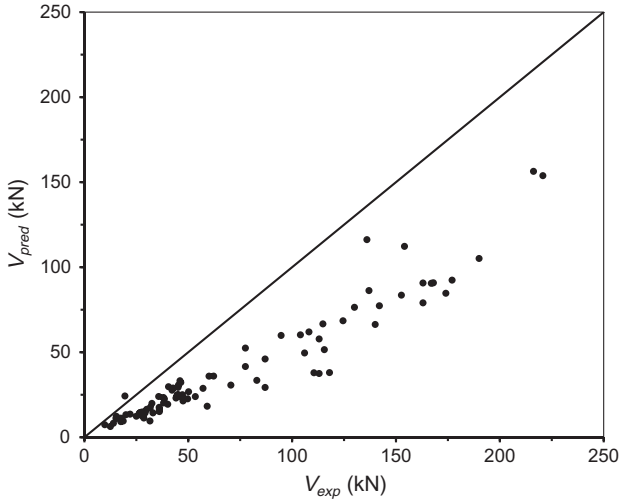

Fig. 1. ACI 440.1R-06 (2007) predicted vs. experimental shear capacities.

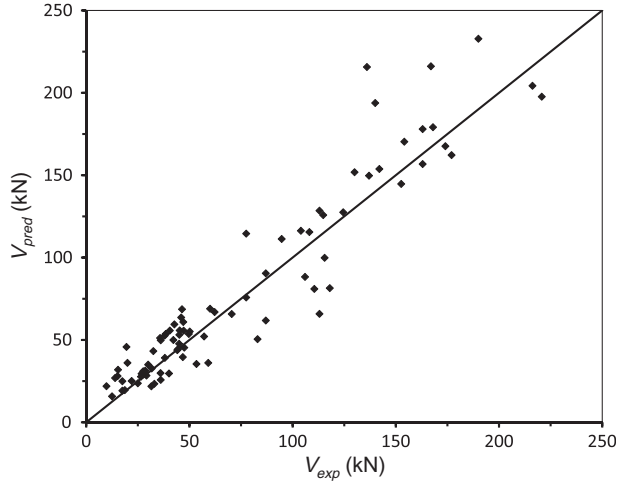

Fig. 2. CNR DT 203/2006 [7] predicted vs. experimental shear capacities.

the design formulas for conventional steel reinforced concrete members after applying some modifications to account for the difference between steel and FRP reinforcement properties. For example, JSCE [22], BISE [5], CNR DT 203/2006 [7], ISIS-M03-07 [21], Tottori and Wakui [36] apply a correction factor E_f/E_s that takes into account the difference in the elastic modulus between FRP, E_f, and steel reinforcement, E_s. However, this modification factor E_f/E_s is raised to different powers in these guidelines. On the other hand, the modification proposed by the ACI-440.1R-06 [1], CAN/CSA-S806-02 [6], Razaqpur and Isgor [32] and El-Sayed et al. [12] only includes the FRP reinforcement axial rigidity $E_f A_f$.

Table 2
Summary of statistical results for shear design methods.

Design method	Mean	Standard deviation	*COV* (%)	*MAE* (%)
ACI 440.1R-06 [1]	1.894	0.443	23.37	44.95
CNR DT 203/2006 [7]	0.954	0.261	27.41	24.28
ISIS-M03-07 [21]	1.353	0.416	30.77	30.11

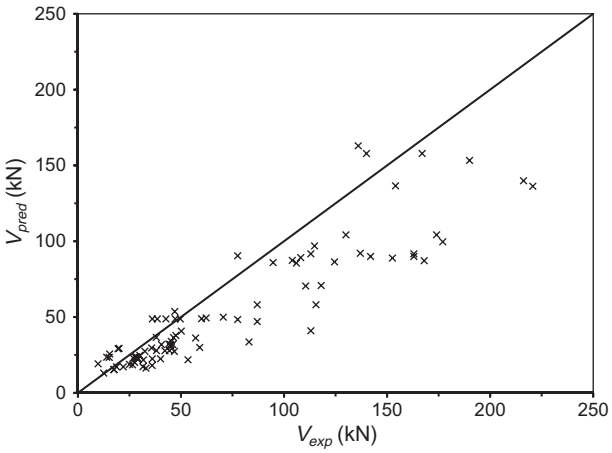

Fig. 3. ISIS-M03-07 [21] predicted vs. experimental shear capacities.

Many published provisions and methods for shear resistance of FRP reinforced concrete members [1,5-7,13,21,22,32,33,39] have been considered in this study i.e. the latest versions and those which are currently implemented around the world. However, for the sake of brevity, only three methods are assessed and presented here, namely provisions developed by ACI-440.1R-06 [1], CNR DT 203/2006 [7] and ISIS-M03-07 [21]. It is also to be noted that in these design provisions, all safety factors were ignored, i.e. assigned to 1.0. In reality safety factors would be applied to make shear capacity predictions more conservative and acceptable for design purposes.

2.1. ACI-440.1R-06 shear design provisions

ACI-440.1R-06 [1] adopted the design method proposed by Tureyen and Frosch [38]. The ACI-440 shear capacity V_c of FRP reinforced concrete members is given as:

$$V_c = \frac{2}{5}\left(\sqrt{(2\rho_f n_f + (\rho_f n_f))^2} - \rho_f n_f\right)\sqrt{f'_c} b_w d \quad (1)$$

where $n_f = \frac{E_f}{E_c}$ is the modular ratio, E_f and $E_c (= 4.7\sqrt{f'_c}$ in GPa) are FRP and concrete elastic moduli, respectively, $\rho_f = \frac{A_f}{b_w d}$ is the FRP reinforcement ratio, A_f is the FRP reinforcement area, b_w and d are the width and effective depth of FRP members and f'_c is the cylinder compressive strength of concrete (in MPa). The above equation is

Table 1
Distribution of geometrical and mechanical properties of the 87 test specimens.

Web width b_w		Effective depth d		Concrete compressive strength f'_c		Shear span to depth ratio a/d		Modulus of elasticity E_f		Reinforcement ratio ρ_f (%)	
Range (mm)	Freq.	Range (mm)	Freq.	Range (MPa)	Freq.	Range	Freq.	Range (GPa)	Freq.	Range	Freq.
80–100	1	100–200	23	20–30	11	2.48–3.0	11	20–50	56	0.25–0.75	26
100–200	28	200–300	34	30–40	26	3.0–3.5	38	50–80	3	0.75–1.25	23
200–300	33	300–400	26	40–50	30	3.5–4.0	10	80–110	3	1.25–1.75	20
300–400	7	400–500	0	50–60	6	4.0–4.5	11	110–140	18	1.75–2.25	11
400–500	10	500–600	0	60–70	8	4.5–5.0	1	140–170	6	2.25–2.75	6
500–1000	8	600–1000	4	70–90	6	5.0–6.5	16	170–200	1	2.75–3.25	1

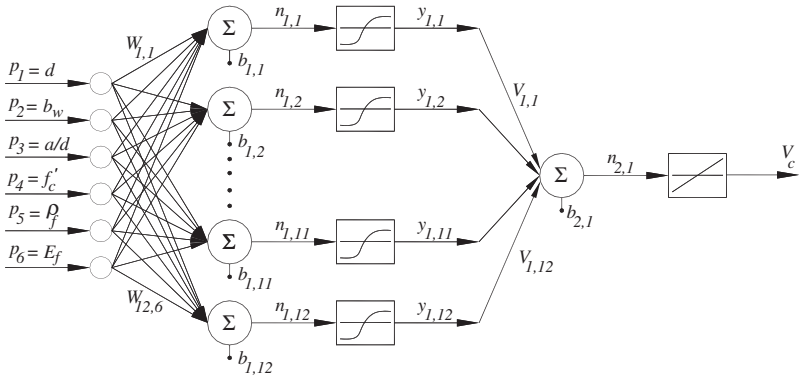

Fig. 4. Architecture of $6 \times 12 \times 1$ network.

simply the ACI-318 shear equation for steel reinforced concrete modified by a factor to account for the axial stiffness of FRP reinforcement.

2.2. CNR DT 203/2006 shear capacity approach

The CNR DT 203 Task Group [7] conducted a calibration to adjust the shear resistance equation of steel reinforced concrete members in Eurocode 2 [15] and extend it to concrete members reinforced with FRP; the following expression for the shear resistance V_c of FRP reinforced concrete members was proposed:

$$V_c = 1.3\left(\frac{E_f}{E_s}\right)^{\frac{1}{2}}\tau_{rd}k_d(1.2+40\rho_f)b_w d \tag{2}$$

where $\tau_{rd} = 0.25f_{ckt0.05}$ is the design shear stress, $f_{ckt0.05}(=0.7f_{ctm})$ is the characteristic tensile strength of concrete (5% fractile), $f_{ctm}(=0.3(f'_c))^{\frac{2}{3}}$ is the mean value of concrete tensile strength, E_s is the steel elastic modulus and $k_d(=1.6-d \geqslant 1.0$, $d =$ depth in metres) is a size effect parameter. The above equation was calibrated for FRP reinforcement ratios ρ_f in the range: $0.01 < \rho_f < 0.02$. The motivation behind Eq. (2) was based on the objective of developing a simple and reliable equation having a structure with which practitioners are familiar [16].

2.3. ISIS-M03-07 shear design method

The shear strength of members reinforced with FRP bars in ISIS-M03-07 [21] is determined in accordance to the same principles for steel reinforced concrete in CSA A23.3-94 [4] after accounting for the difference in the elastic modulus between steel and FRP reinforcement. The shear strength formula distinguishes between members with effective depth d less or greater than 300 mm as given below:

$$V_c = 0.2\lambda\sqrt{f'_c}b_w d\left(\frac{E_f}{E_s}\right)^{\frac{1}{2}} \quad d \leq 300\ \text{mm} \tag{3a}$$

$$V_c = \left(\frac{260}{1000+d}\right)\lambda\sqrt{f'_c}b_w d\left(\frac{E_f}{E_s}\right)^{\frac{1}{2}} \geq 0.1\lambda\sqrt{f'_c}b_w d\left(\frac{E_f}{E_s}\right)^{\frac{1}{2}}$$
$$d > 300\ \text{mm} \tag{3b}$$

where λ is a factor accouting for concrete density (assumed 1.0 in this study).

3. Experimental database

An experimental database of 138 FRP reinforced concrete members failed in shear was initially created to compare experimentally determined shear capacities with the predictions of the three shear design methods presented above, and also to train and test NNs to be developed for shear capacity prediction. The database was then refined to 87 specimens as explained below. 5 of the 138 test specimens collected had shear span to depth ratios a/d less than 2.4 constituting deep beams and 2 specimens with a/d more than 6.5 identified to be very long beams; these 7 specimens were omitted as they are not compatible with the majority of the database specimens. In addition, most of the current shear design methods were developed mainly on the testing of slender beams and not deep or long beams. A few of the specimens collected from the same investigation had the same material and geometrical properties, however, their experimentally obtained shear capacities were different. Therefore, the shear capacities of specimens with identical geometrical and material properties have been averaged to reduce the noise in the training samples and consequently achieve successful training and generalisation of NNs created.

The material and geometrical properties of the 87 members in the refined database as well as their original sources are given in Appendix A (Table A.1). Of the 87 test specimens, 77 were beams and the other 10 were one way slabs. All specimens in the database were simply supported, tested in either three or four points loading arrangement, had no transverse reinforcement and failed in shear. The distribution of geometrical and mechanical properties of the 87 test specimens is given in Table 1.

3.1. Comparisons between current design methods and experiments

Table A.1 in Appendix A gives the ratio of experimentally measured shear capacity V_{exp} to that predicted by the three design methods, V_{pred}, for every specimen in the refined database. For each shear design method, four statistical observations are also

Table 3
Statistical results for 10 NNs created.

NN architecture[a]	Mean	Standard deviation	*COV* (%)	MAE (%)
$6 \times 3 \times 1$	1.032	0.240	23.24	15.33
$6 \times 6 \times 1$	1.021	0.200	19.61	13.11
$6 \times 10 \times 1$	1.020	0.211	20.68	13.87
$6 \times 12 \times 1$	1.018	0.189	18.57	12.83
$6 \times 15 \times 1$	1.020	0.182	17.82	13.03
$6 \times 21 \times 1$	1.024	0.216	21.09	14.02
$6 \times 3 \times 3 \times 1$	1.023	0.216	21.16	15.17
$6 \times 3 \times 5 \times 1$	1.022	0.214	20.90	14.96
$6 \times 5 \times 5 \times 1$	1.012	0.190	18.75	14.29
$6 \times 6 \times 1 \times 1$	1.019	0.179	17.60	13.14

[a] The first and last numbers indicate the number of neurons in input and output layers, respectively, and the others refer to the number of neurons in hidden layers.

Table 4
Garson index values for NN input parameters.

Input parameter	d	b_w	a/d	f'_c	ρ_f	E_f
Garson index (relative importance)	0.1833	0.1618	0.0965	0.1418	0.2006	0.2160

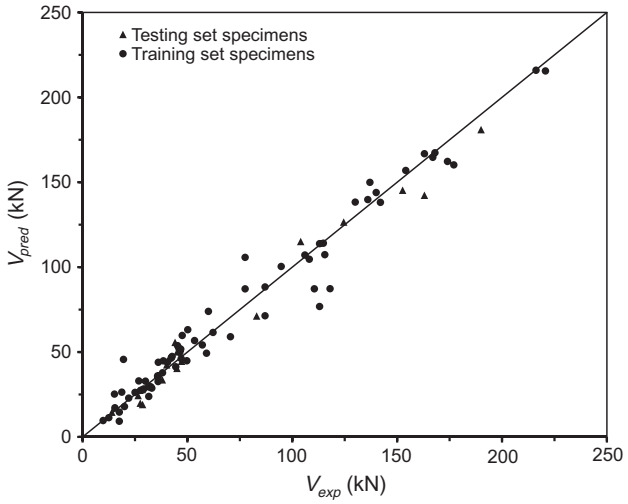

Fig. 5. $6 \times 12 \times 1$ network predicted vs. experimental shear capacities.

calculated to assess the predicted shear capacities to those experimentally observed, namely the mean, standard deviation, coefficient of variation (*COV*%) and mean absolute square percentage error (*MAE*%); these statistical parameters are summarised in Table 2. Verification of the shear design equations is also shown by plotting the predicted shear strengths against the experimental values for all specimens in Figs. 1–3. In each plot a straight line, with $V_{exp} = V_{pred}$, is drawn. The ACI-440.1R-06 is the most conservative, even though all safety factors were not considered, and also shows the largest scatter of results. On the other hand, CNR DT 203/2006 is the most accurate among the three methods with a mean of 0.954 and least scatter with a standard deviation of 0.261.

4. Artificial neural network modelling

Artificial neural networks (NNs) are defined as computing systems made up of a number of simple, highly interconnected processing elements called neurons. They can be applied to complex problems described with a large amount of data, where rational engineering solutions have not yet been developed, such as the problem in hand.

4.1. Multi layered feed forward NNs

A typical multi-layered feed-forward NN without input delay commonly consists of an input layer, one or more hidden layers and an output layer as shown in Fig. 4, where p indicates the input vector, w and v give the weight matrices for input and hidden layers and b represents the bias vector. n is the net input passed to the transfer function f to obtain the neuron's output vector y. Input data of input layer given from outside feed into hidden layers connecting input and output layers in a forward direction, and then useful characteristics of input data are extracted and remembered in hidden layers to predict the output. Finally NN predictions are produced through the output layer. Each processing element usually has many inputs, but it can send out only one output.

Back propagation is generally known to be the most powerful and widely used technique to train a network. To obtain some desired outputs, weights, which represent connection strength between neurons, and biases, are adjusted using a number of training inputs and the corresponding target values. The network error, that is the difference between calculated and expected target patterns, is then back propagated from the output layer to the input layer to update the network weights and biases. The process of adjusting neuron weights and biases is conducted until the network error arrives at a specific level of accuracy.

The input and output neurons are defined by the problem to be solved whereas the number of hidden layers and the corresponding number of neurons per layer may be determined by trialling different configurations until reaching the optimum. The NN toolbox available in MATLAB R2010a [24] was used for creating the current NN models.

4.2. Inputs and outputs of developed NN

Based on the experimental observations and recently developed formulae [1,5–7,13,21,22,32,33,39], the following parameters are used as the inputs of the networks to be developed: d, b_w, a/d, f'_c, ρ_f and E_f, where various notations are defined in Table 1. The output is the shear capacity V_c of FRP reinforced concrete members.

The refined database of 87 specimens is used for training and testing NNs. As mentioned earlier in the paper, many gathered specimens have exact same parametric values i.e. material and geometrical properties but the experimentally measured shear capacities are different, so the experimentally obtained shear capacities of these specimens have been averaged. Based on initial trial and error testing it was realised that the averaged database of 87 specimens allowed the NNs to generalise better and train more efficiently than using the original un-averaged database.

4.3. Generalisation of NN

One of the problems that occur during NN training is the so called over fitting as the network may memorise the training features, but not learn to generalise new patterns [9]. One of the most

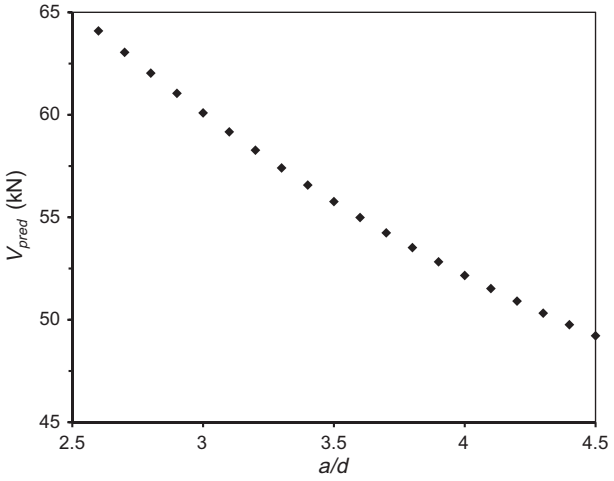

Fig. 6. Shear span to depth ratio, a/d, effect on shear capacity.

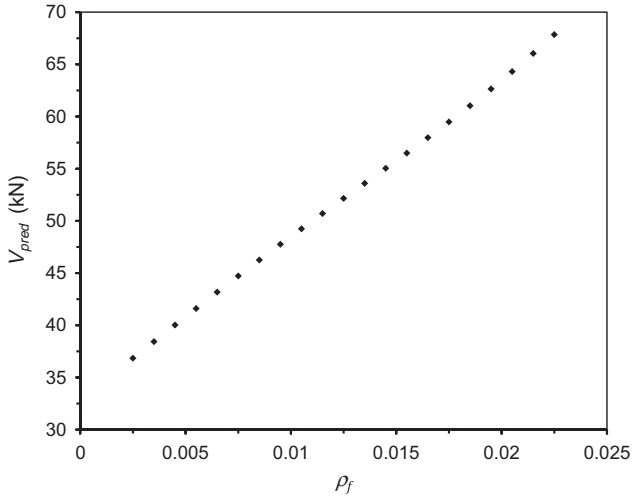

Fig. 7. FRP reinforcement ratio, ρ_f, effect on shear capacity.

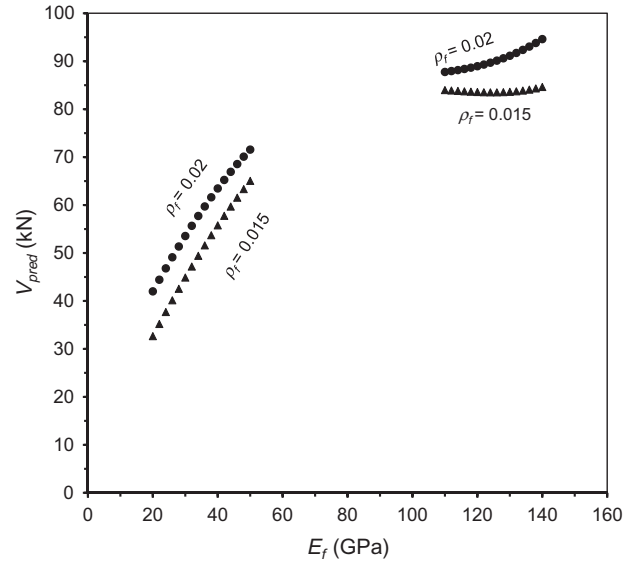

Fig. 8. FRP elastic modulus, E_f, effect on shear capacity.

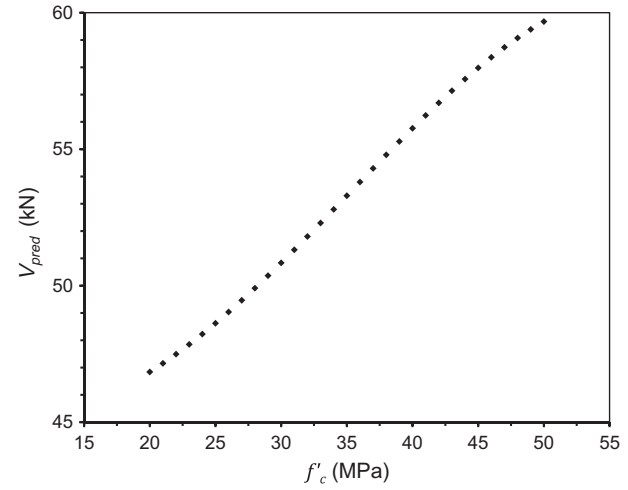

Fig. 9. f'_c effect on shear capacity.

effective and widely used techniques to improve generalisation of NNs is early stopping. In this technique, the available data are divided into three subsets: training, validation and test subsets. The training set is used for computing the gradient and updating the network weights and biases to diminish the training error. When the error on the validation set, which is monitored during the training process, increases for a specified number of iterations, the training is stopped, and then the network weights and biases at the minimum validation error are returned. The test set error is not used during training, but it is used for verification of the NNs [9]. However for the current problem, this early stopping technique has shown to be inefficient and thus not most suitable.

On the other hand, Bayesian regularisation (BR) is known to provide better generalisation performance than early stopping technique when the dataset is relatively small [9], such as the case in this paper, as it does not require that a validation data set be separate from the training data set. Therefore, BR has been adopted in the current development. Hence, all database specimens are divided into only two subsets: training and testing as detailed later. Equivalent to the early stopping technique, the training set is used for computing the gradient and updating the network weights and biases to diminish the training error.

The training algorithm is allowed to run until convergence i.e. when the sum squared error (*SSE*) is relatively constant over several iterations as calculated by the equation below:

$$SSE = \sum_{i=1}^{m} (V_{i,pred} - V_{i,exp})^2 \quad (4)$$

where m is the total number of training specimens. Then the testing subset is used to assess the created network and any possible complications due to over fitting. For this investigation, 80% is used for training and 20% for testing the networks as indicated in Table A.1. Over fitting in training and outputs of NNs is commonly influenced by the number of hidden layers and neurons in each hidden layer. A trial and error approach was therefore carried out to choose an optimum number of hidden layers and number of neurons in each hidden layer as explained later.

In a multi-layered feed-forward NN having a back-propagation algorithm, the combination of non-linear and linear transfer functions can be trained to approximate any function arbitrarily well [9]. For the NNs created in this study, tan-sigmoid transfer function was employed in the hidden layers as it is generally known to be more suitable for multi-layer networks developed for non-linear applications than log-sigmoid function that generates outputs between 0 and 1 [9]. On the other hand, linear transfer function was adopted in the output layer; its suitability was also reiterated by the trial and error experiments conducted.

4.4. Data normalisation

By performing certain pre-processing steps on the network inputs and targets, NN training can be made more efficient, commonly referred to as normalisation. As upper and lower bounds of the tan-sigmoid function output are +1 and −1, respectively, inputs and targets in the database were normalised so that they fall in the interval [−1, 1]. The network output is then reverse transformed back into the units of the original target data when the created network is simulated. Most of the network creation functions in the NN toolbox of Matlab automatically assign pre and post processing functions to the network inputs and targets. Initial weights and biases were randomly assigned by the NN toolbox of Matlab. The maximum number of iterations (epochs) was set at 1000. In the training process of the multi-layer feed-forward NNs developed, the error between the prediction of the output layer and experimental shear strength was then back propagated from the output layer to the input layer in which the connection weights

and biases were adjusted. The training process was repeated until the maximum epochs were reached, the *SSE* converged or the performance gradient fell below a minimum value. However, the *SSE* converged in most trials.

4.5. NN training and testing

Of the 87 specimens (refined database), 80% (70 specimens) of data was assigned to training and 20% (17 specimens) to testing as given in Table A.1. The distribution of each parameter across its range in the training subset was manually examined to ensure that it covers a good spread within the range considered. At early stages of trial and error network creation and testing, data corresponding to a high error for the test set were moved into the training set and replaced in the test set with another random combination to achieve better results and learning.

4.6. Comparisons of NN predictions and experimental shear capacities

A total of 10 different NNs with different architectures were created and tested i.e. networks with varying number of hidden layers and corresponding neurons as listed in Table 3. Each created network weights and biases were randomly re initialised nine times thus the results shown are the most favourable of the ten trials for each NN architecture. *SSE* defined in Eq. (4) was used to monitor the network performance. For each NN four statistical observations; mean, standard deviation, *COV*% and *MAE*% of V_{exp}/V_{pred} are used to assess predicted to experimentally observed shear capacities for all specimens as presented in Table 3.

Although the mean and standard deviation of the ratio of predicted and measured shear capacities of FRP reinforced concrete members presented in Table 3 were similar for different NN architectures, the $6 \times 12 \times 1$ NN was finally selected for predicting shear capacity. In addition, over-fitting seldom occurred in the $6 \times 12 \times 1$ network due to its simpler architecture and better predictions especially for the testing data set compared with NNs having more neurons or hidden layers. It was also evident that the $6 \times 12 \times 1$ NN is able to predict a smooth trend for inputs considered in the parametric study presented below. Fig. 5 compares the $6 \times 12 \times 1$ network prediction and experimental results. It indicates generalisation and good modelling of the problem with low scatter around the diagonal line showing consistency and efficiency.

The fact that the somewhat limited training set of 70 specimens was successful for developing networks which provide accurate predictions of shear capacity suggests that the problem is not heavily non-linear. This is also reiterated by the fact that the problem can be modelled reasonably well with a single hidden layer and a relatively small number of corresponding neurons.

Comparing the predictions from the $6 \times 12 \times 1$ NN and existing shear design methods presented in sections 2.1, 2.2 and 2.3 for the specimens in the database, the following observations can be made:

- The NN has a mean value closer to 1, indicating its superior average accuracy as compared to the design methods.
- The NN standard deviation, *COV*% and *MAE*% are far much lower than those of the three design methods. Graphically the NN also shows more favourable results. The data points are less scattered and closer to the diagonal line indicating that the NN predictions are more accurate and consistent at predicting shear resistance.

5. Parametric analysis using developed NN

The trained $6 \times 12 \times 1$ NN is used to analyse the influence of the main parameters on shear capacity of FRP reinforced concrete members. This has been done via two avenues; firstly the Garson index [18] which identifies the relative importance of each parameter based on the created NN weightings at node points and secondly by using the created network to simulate indicative results for the influencing parameters.

5.1. Garson index of trained NN

The Garson index [18] has been used to identify the relative importance of all input parameters with respect to the shear resistance as the output parameter via operations between the weight matrices generated in two successive layers of the trained NN. For a NN with one hidden layer the Garson index is determined from the following formula:

$$G_{ik} = \frac{\sum_{j=1}^{J} \frac{|W_{ij}||V_{jk}|}{\sum_{i=1}^{I}|W_{ij}|}}{\sum_{i=1}^{I}\sum_{j=1}^{J} \frac{|W_{ij}||V_{jk}|}{\sum_{i=1}^{I}|W_{ij}|}} \quad (5)$$

where G_{ik} indicates the connectivity strength between the i^{th} parameter of the input layer and the k^{th} prediction of the output layer; $|W_{ij}|$ is the weight matrix linking the I neurons of the input layer with the J neurons of the intermediate hidden layer, $|V_{jk}|$ represents the weight matrix linking the J neurons of the intermediate hidden layer with the K neurons of the output layer, as shown in Fig. 4.

Table 4 gives the Garson index values for the six input parameters considered in the final NN configuration ($6 \times 12 \times 1$). It is clear that all parameters have a high relative importance which demonstrates their usage as input parameters for the NNs and shear design methods. ρ_f and E_f have a relatively large weighting, shortly followed by d, then b_w and then f'_c. The lowest relative importance is that of a/d, approximately half that of d, ρ_f and E_f. This may be attributed to the range of a/d in the refined database used to train and test NNs. The literature shows that a/d has a large effect for deeper beams ($0 < a/d < 2.5$) than it does for slender beams ($2.5 < a/d < 6.5$) similar to those in the refined database.

5.2. Parametric analysis

The developed $6 \times 12 \times 1$ network is employed to examine the effect of the main input parameters on shear capacity. The ranges of the inputs have shown that there are parts which are covered by a limited amount of specimens, if any, mainly due to the fact that many tests have not been conducted so as to have ranges which are fully and thoroughly covered as presented in Table 1. Therefore only parts of the ranges which are appropriately covered are considered in this parametric study to give reliable trends in the confidence that the NN has generalised for those parts accordingly. The values, at which various parameters were kept constant when other parameters were being changed in the analysis, are: $d = 300$ mm; $b_w = 200$ mm; $a/d = 3.5$; $f'_c = 40$ MPa; $p_f = 1.5\%$ and $E_f = 40$ GPa. These values have been chosen as they are not at the extremes of the whole range for each parameter and also occur within the band for which there is a high frequency.

5.2.1. Effect of shear span to depth ratio

The influence of the shear span to depth ratio a/d is presented in Fig. 6. It is clear that as a/d increases, shear capacity decreases. This is in accordance with the known effect of a/d on reinforced concrete shear capacity indicating that the NN has modelled the problem adequately. Interestingly most shear design methods do not consider a/d to be a notable influencing parameter.

Table A.1
Refined experimental database of 87 specimens and shear strength predictions.

Source	Specimen No.	b_w (mm)	d (mm)	a/d	f'_c (MPa)	ρ_f (%)	E_f (GPa)	V_{exp} (kN)	V_{exp}/V_{pred}			
									ACI 440.1R-06 [1]	CNR DT 203/2006 [7]	ISIS-M03-07 [21]	$6 \times 12 \times 1$ NN
El-Sayed et al. [11]	1	1000	165.3	6.0	40.0	0.39	114	140	2.11	0.72	0.89	0.97
	2	1000	165.3	6.0	40.0	0.78	114	167	1.84	0.77	1.06	1.01
	3[a]	1000	160.5	6.2	40.0	1.18	114	190	1.81	0.82	1.24	1.05
	4	1000	162.1	6.2	40.0	0.86	40	113	1.95	0.88	1.23	0.99
	5	1000	159	6.3	40.0	1.70	40	142	1.84	0.92	1.58	1.03
	6[a]	1000	162.1	6.2	40.0	1.71	40	163	2.06	1.04	1.78	1.15
	7	1000	159	6.3	40.0	2.44	40	163	1.80	0.92	1.81	0.98
	8	1000	154.1	6.5	40.0	2.63	40	168	1.85	0.94	1.93	1.00
El-Sayed et al. [13]	9	250	326	3.1	50.0	0.87	128	77.5	1.48	0.68	0.86	0.73
	10	250	326	3.1	50.0	0.87	39	70.5	2.30	1.07	1.41	1.19
	11[a]	250	326	3.1	44.6	1.24	134	104	1.73	0.89	1.19	0.90
	12	250	326	3.1	44.6	1.22	42	60	1.67	0.87	1.23	0.81
	13[a]	250	326	3.1	43.6	1.72	134	124.5	1.82	0.98	1.44	0.98
	14	250	326	3.1	43.6	1.71	42	77.5	1.86	1.02	1.60	0.89
El-Sayed et al. [12]	15	250	326	3.1	63.0	1.71	135	130	1.70	0.86	1.25	0.94
	16	250	326	3.1	63.0	1.71	42	87	1.89	0.96	1.50	0.98
	17	250	326	3.1	63.0	2.2	135	174	2.05	1.04	1.67	1.07
	18	250	326	3.1	63.0	2.2	42	115.5	2.24	1.16	1.99	1.08
Razaqpur et al. [31]	19	200	225	2.7	40.5	0.25	145	36.1	2.19	0.72	0.74	0.82
	20	200	225	2.7	49.0	0.5	145	47	1.97	0.77	0.88	1.02
	21[a]	200	225	2.7	40.5	0.63	145	47.2	1.89	0.85	0.97	1.06
	22	200	225	2.7	40.5	0.88	145	42.7	1.48	0.72	0.88	0.90
	23	200	225	3.6	40.5	0.5	145	49.7	2.20	0.93	1.02	1.11
	24	200	225	4.2	40.5	0.5	145	38.5	1.70	0.72	0.79	0.86
Gross et al. [20]	25–27[c]	127	143	6.4	60.3	0.33	139	13.97	1.69	0.52	0.59	0.96
	28–30[b]	159	141	6.5	61.8	0.58	139	19.97	1.51	0.55	0.68	1.12
	31–33[b]	89	143	6.4	81.4	0.47	139	9.8	1.33	0.45	0.51	1.01
	34–36[b]	121	141	6.5	81.4	0.76	139	15.4	1.25	0.48	0.60	0.90
Tariq and Newhook [35]	37–38[b]	160	346	2.8	37.3	0.72	42	59.1	3.24	1.64	1.97	1.20
	39–40[c]	160	346	3.3	43.2	1.1	42	44.1	1.91	1.01	1.37	0.79
	41–42[b]	160	325	3.5	34.1	1.54	42	46.8	1.98	1.18	1.71	0.90
	43–44[b]	130	310	3.1	37.3	0.72	120	47.5	2.22	1.05	1.26	0.79
	45–46[b]	130	310	3.7	43.2	1.1	120	50.15	1.87	0.91	1.23	0.79
	47–48[b]	130	310	3.7	34.1	1.54	120	57.1	1.98	1.10	1.58	1.05
Gross et al. [19]	49–51[c]	203	225	4.1	79.6	1.25	40.3	38.03	1.63	0.72	1.04	1.13
	52–54[b]	152	225	4.1	79.6	1.66	40.3	32.5	1.63	0.75	1.19	1.10
	55–57[b]	165	224	4.1	79.6	2.1	40.3	35.77	1.49	0.70	1.21	0.99
	58–60[b]	203	224	4.1	79.6	2.56	40.3	46.4	1.44	0.68	1.27	0.93
Tureyen and Frosch [37]	61	457	360	3.4	39.7	0.96	40.5	108.1	1.74	0.94	1.21	1.03
	62	457	360	3.4	39.7	0.96	37.6	94.7	1.58	0.85	1.10	0.94
	63	457	360	3.4	40.3	0.96	47.1	114.8	1.72	0.91	1.18	1.01
	64	457	360	3.4	42.3	1.92	40.5	137	1.59	0.92	1.49	0.91
	65[a]	457	360	3.4	42.5	1.92	37.6	152.6	1.83	1.05	1.72	1.05
	66	457	360	3.4	42.6	1.92	47.1	177	1.92	1.09	1.78	1.10
Yost et al. [41]	67–69[b]	229	225	4.1	36.3	1.11	40.3	38.1	1.89	0.97	1.37	1.01
	70–72[b]	178	225	4.1	36.3	1.42	40.3	31.73	1.81	0.97	1.46	1.08
	73–75[b]	229	225	4.1	36.3	1.66	40.3	44.43	1.83	1.00	1.59	1.08
	76–78[b]	279	225	4.1	36.3	1.81	40.3	45.27	1.48	0.81	1.33	0.84
	79–81[c]	254	224	4.1	36.3	2.05	40.3	45.1	1.54	0.85	1.47	0.90
	82–84[b]	229	224	4.1	36.3	2.27	40.3	42.2	1.52	0.84	1.52	0.91

Alkhrdaji et al. [2]	85	178	279	2.7	24.1	2.3	40	53.4	2.23	1.51	2.45	0.94
	86	178	287	2.6	24.1	0.77	40	36.1	2.39	1.40	1.61	1.01
	87[a]	178	287	2.6	24.1	1.34	40	40.1	2.07	1.35	1.79	0.95
Deitz et al. [8]	88	305	157.5	4.5	28.6	0.73	40	26.8	1.85	0.91	1.17	0.81
	89	305	157.5	5.8	30.1	0.73	40	28.3	1.92	0.93	1.20	1.03
	90	305	157.5	5.8	27.0	0.73	40	29.2	2.04	1.03	1.31	1.03
	91[a]	305	157.5	5.8	28.2	0.73	40	28.5	1.97	0.97	1.25	1.02
	92	305	157.5	5.8	30.8	0.73	40	27.6	1.86	0.89	1.16	1.01
Mizukawa et al. [26]	93	200	260	2.7	34.7	1.3	130	62.2	1.73	0.93	1.26	1.01
Duranovic et al. [10]	94	150	210	3.7	32.9	1.31	45	22	1.62	0.88	1.28	0.96
	95[a]	150	210	3.7	38.1	1.31	45	26.5	1.87	0.96	1.44	1.09
Swamy and Aburawi [34]	96	254	222	3.2	39.0	1.55	34	19.5	0.80	0.43	0.67	0.43
Zhao et al. [42]	97[a]	150	250	3.0	34.3	1.51	105	45	1.79	0.94	1.41	1.11
	98	150	250	3.0	34.3	3.02	105	46	1.38	0.72	1.45	0.89
	99	150	250	3.0	34.3	2.27	105	40.5	1.36	0.73	1.27	0.92
Lubell et al. [23]	100	450	970	3.1	40.0	0.46	40	136	1.17	0.63	0.83	0.97
Ashour [3]	101	150	171	3.9	34.0	0.45	38	12.5	1.98	0.79	0.96	1.10
	102	150	218	3.1	34.0	0.71	32	17.5	1.90	0.91	1.15	1.20
	103	150	268	2.5	34.0	0.86	32	25	2.02	1.06	1.33	0.95
	104	150	168	4.0	59.0	1.39	32	17.5	1.56	0.70	1.13	1.89
	105[a]	150	218	3.1	59.0	1.06	32	27.5	2.14	0.95	1.37	1.38
	106	150	268	2.5	59.0	1.15	32	30	1.83	0.86	1.21	0.91
Tottori and Wakui [36]	107–108[b]	200	325	3.2	44.6	0.7	137	110.5	2.91	1.36	1.57	1.27
	109	200	325	3.2	45.0	0.7	137	118	3.10	1.45	1.67	1.35
	110–112[b]	200	325	3.2	46.9	0.9	192	106	2.14	1.20	1.24	0.99
	113–115[b]	200	325	3.2	46.9	0.9	58	87	2.97	1.41	1.85	1.22
Nagasaka et al. [27]	116	250	265	3.1	34.1	1.9	56	113	3.01	1.72	2.76	1.47
	117[a]	250	265	3.1	22.9	1.9	56	83	2.48	1.64	2.47	1.17
Nakamura and Higai [28]	118	300	150	4.0	22.7	1.3	29	33	2.30	1.41	2.02	1.15
	119	300	150	4.0	27.8	1.8	29	36	2.05	1.20	1.99	1.10
Matta et al. [25]	120	457	883	3.1	29.5	0.59	40.7	154.1	1.37	0.90	1.13	0.98
	121	457	880	3.1	29.5	1.18	40.7	220.7	1.43	1.12	1.62	1.02
	122	456	880	3.1	30.7	1.18	41.4	216.2	1.38	1.06	1.55	1.00
	123	114	294	3.1	59.7	0.59	40.8	15.2	1.35	0.54	0.65	0.60
	124–125[b]	114	294	3.1	32.1	0.59	40.8	18.7	1.96	0.96	1.09	0.71
	126[a]	229	147	3.1	59.7	0.59	40.8	28.6	2.53	0.91	1.22	1.50
	127–128[b]	229	147	3.1	32.1	0.59	40.8	31.55	3.29	1.44	1.83	1.32

[a] Specimens used for testing NNs.
[b] Specimens having the same geometrical and material properties.
[c] Specimens used for testing NNs and having the same geometrical and material properties.

5.2.2. Effect of longitudinal reinforcement ratio

Fig. 7 shows that V_c increases with increasing longitudinal FRP reinforcement ratio ρ_f, which is general knowledge in the field. The NN indicates that V_c is almost linearly proportional to ρ_f, disputing the assumptions made by some of the shear design methods that it is proportional to $\rho_f^{1/2}$ or $\rho_f^{1/3}$. Surprisingly some design methods, for example ISIS-M03-07 [21], do not even consider ρ_f in their shear capacity formula.

5.2.3. Effect of elastic modulus

The influence of FRP elastic modulus E_f is presented in Fig. 8. This figure has been produced for the most commercially available ranges of E_f (≈20–50 and 110–140 GPa) and consequently used in NN training. However, as future shear test data become available in the E_f range between 50 and 110 GPa, the NN will be re-trained to cover the entire E_f range between 20 and 140 GPa. The figure shows that for smaller E_f values (20–50 GPa), V_c increases with increasing E_f, however, for higher E_f values (110–140 GPa), the effect of increasing E_f has a much lesser influence on V_c, if any. None of the empirically developed shear design methods presented in the literature takes this dual effect into account; the formulas are the same regardless of whether high modulus CFRP or lower modulus GFRP or AFRP bars are used as flexural tensile reinforcement.

5.2.4. Effect of concrete compressive strength

The effect of increasing concrete compressive strength f_c' is to increase V_c as depicted in Fig. 9. A fitting function analysis was conducted to evaluate the power of f_c' that achieves the best fit of the data presented in Fig. 9. It was found that f_c' raised to a power of 1/4 best describes the trend when $f_c' < 35$ MPa; however, a power of 1/3 shows a better correlation for $f_c' > 35$ MPa, agreeing with most shear design methods in the literature.

6. Conclusions

Based on the above investigation, the following conclusions may be drawn:

- The ACI-440.1R-06 and ISIS-M03-07 were not accurate at predicting shear capacity and had a large dispersion of data about the mean. However, CNR DT 203/2006 design method showed reasonable accuracy and scatter in calculating shear resistance.
- The shear capacity of FRP reinforced concrete members is not heavily non-linear as it can be modelled reasonably well with a single hidden layer and small number of corresponding neurons e.g. $6 \times 3 \times 1$ network. In addition, NN training was successfully achieved using a limited training set of 70 specimens.
- Statistically and graphically the NN proved to be considerably more accurate than the three design methods considered with its better mean and proved to be more consistent with its lower standard deviation and graphical scatter, at predicting the shear capacity of FRP reinforced concrete members.
- The Garson indices calculated for the trained NN clearly showed that all parameters considered have a high relative importance demonstrating their usage as input parameters for the NN. For the parameter ranges used to develop NNs, FRP reinforcement amount and modulus of elasticity have the highest weighting, shortly followed by the beam depth, then width and then concrete compressive strength. The shear span to depth ratio has the lowest relative importance for the range (a/d = 2.49–6.49) studied.
- The trained NN predicted that the shear capacity is:
  - proportional to the concrete compressive strength, f_c', raised to a power between 1/4 and 1/3 as assumed by most shear design methods.
  - more linearly proportional to the FRP reinforcement ratio, ρ_f, disputing the assumptions made by few shear design methods that it is proportional to $\rho_f^{1/2}$ or $\rho_f^{1/3}$.
  - proportional to E_f for smaller values of FRP elastic modulus (E_f = 20–50 GPa). However, for higher E_f values (110–140 GPa), the effect of increasing E_f has a much smaller influence on shear capacity, if any. None of the shear design methods take this dual effect into account.
  - Inversely proportional to the shear span to depth ratio a/d that was not considered by most shear design methods.
- The developed network is trained to generalise well within the range of inputs considered. However, it does not have the ability to accurately extrapolate beyond this range.

Acknowledgements

The authors would like to express their dearest appreciation to the financial support provided by the IStructE and Robinson Design Group.

Appendix A

See Table A.1.

References

[1] American Concrete Institute (ACI) Committee 440. Guide for the design and construction of structural concrete reinforced with FRP Bars. ACI 440.1R-06. Farmington Hills (MI): American Concrete Institute; 2006. p. 44.
[2] Alkhrdaji T, Wideman M, Belarbi A, Nanni A. Shear strength of GFRP RC beams and slabs. In: Proceedings of the international conference, composites in construction-CCC 2001, Porto/Portugal; 2001. p. 409–14.
[3] Ashour AF. Flexural and shear capacities of concrete beams reinforced with GFRP bars. Constr Build Mater 2005;20(10):1005–15.
[4] Bentz EC, Collins MP. Development of the 2004 CSA A23.3 shear provisions for reinforced concrete. Can J Civil Eng 2006;33(5):521–34.
[5] British Institution of Structural Engineers (BISE). Interim guidance on the design of reinforced concrete structures using fiber composite reinforcement, IStructE, SETO Ltd., London; 1999.
[6] CAN/CSA S806-02. Design and construction of building components with fibre reinforced polymers. Canadian standards association, Rexdale, Ontario; 2002. p. 177.
[7] CNR-DT 203. Guide for the design and construction of concrete structures reinforced with fiber-reinforced polymer bars. Rome, Italy: National Research Council; 2006.
[8] Deitz DH, Harik IE, Gesund H. One-way slabs reinforced with glass fiber reinforced polymer reinforcing bars. In: Proceedings of the 4th international symposium, fiber reinforced polymer reinforcement for reinforced concrete structures, MI; 1999. p. 279–86.
[9] Demuth H, Beale M. Neural network toolbox for user with MATLAB. USA: The Math Works, Inc.; 2002.
[10] Duranovic N, Pilakoutas K, Waldron P. Tests on concrete beams reinforced with glass fibre reinforced plastic bars. In: Proceedings of the third international symposium on non-metallic (FRP) reinforcement for concrete structures (FRPRCS-3), vol. 2. Sapporo (Japan): Japan Concrete Institute; 1997. p. 479-86.
[11] El-Sayed AK, El-Salakawy E, Benmokrane B. Shear strength of one way concrete slabs reinforced with FRP composite bars. J Compos Constr, ASCE 2005;9(2):147–57.
[12] El-Sayed AK, El-Salakawy E, Benmokrane B. Shear capacity of high- strength concrete beams reinforced with FRP bars. ACI Struct J 2006;103(3):383–9.
[13] El-Sayed AK, El-Salakawy E, Benmokrane B. Shear strength of FRP reinforced concrete without transverse reinforcement. ACI Struct J 2006;103(2):235–43.
[14] El-Sayed AK, Soudki K. Evaluation of shear design equations of concrete beams with FRP reinforcement. J Compos Constr, ASCE 2010;15(1):9–20.
[15] British Standards Institution. Eurocode 2: design of concrete structures – part 1-1: general rules and rules for buildings. BSI, BS EN 1992-1-1:2004; 2004. p. 230.
[16] Fico R, Prota A, Manfredi G. Assessment of Eurocode-like design equations for the shear capacity of FRP RC members. J Compos: Part B 2008;39:792–806.
[17] Flood I, Muszynski L, Nandy S. Rapid analysis of externally reinforced concrete beams using neural networks. Comput Struct 2001;79:1553–9.
[18] Garson GD. Interpreting neural-network connection strengths. AI Expert 1991;6(4):47–51.
[19] Gross SP, Yost JR, Dinehart DW, Svensen E, Liu N. Shear strength of normal and high strength concrete beams reinforced with GFRP reinforcing bars. In: Proc.

of the int. conference on high performance materials in bridges, ASCE; 2003. p. 426–37.
[20] Gross SP, Dinehart DW, Yost JR, Theisz PM. Experimental tests of high-strength concrete beams reinforced with CFRP bars. In: Proceedings of the 4th international conference on advanced composite materials in bridges and structures (ACMBS-4), Calgary, Alberta, Canada, July 20–23; 2004. p. 8.
[21] ISIS Canada. Reinforcing concrete structures with fiber reinforced polymers, ISISM03-07, Canadian network of centers of excellence on intelligent sensing for innovative structures. Manitoba: University of Winnipeg; 2007. p. 151.
[22] Japan Society of Civil Engineers, JSCE. Recommendation for design and construction of concrete structures using continuous fiber reinforcing materials. In: Machida A, editor. Concrete engineering series, vol. 23. Tokyo (Japan); 1997. p. 325.
[23] Lubell A, Sherwrvod T, Bents E, Collins MP. Safe shear design of large wide beams. Concr Int 2004;26(1):67–79.
[24] MATLAB, MATLAB the language of technical computing, student version 2010a. Natwick (MA, USA): MathWorks Inc.; 2010.
[25] Matta F, Nanni A, Hernandez TM, Benmokrane B. Scaling of strength of FRP reinforced concrete beams without shear reinforcement. In: Fourth international conference on FRP composites in civil engineering (CICE2008), Zurich, Switzerland; 2008. p. 6.
[26] Mizukawa Y, Sato Y, Ueda T, Kakuta Y. A study on shear fatigue behavior of concrete beams with FRP rods. In: Proceedings of the third international symposium on non-metallic (FRP) reinforcement for concrete structures (FRPRCS-3), vol. 2. Sapporo (Japan): Japan Concrete Institute; 1997. p. 309–16.
[27] Nagasaka T, Fukuyama H, Tanigaki M. Shear performance of concrete beams reinforced with FRP stirrups. In: Nanni A, Dolan C, editors. ACI SP-138. Detroit, Mich: American Concrete Institute; 1993. p. 789–811.
[28] Nakamura H, Higai T. Evaluation of shear strength of concrete beams reinforced with FRP, concrete library international. Proc Jpn Soc Civil Eng 1995;26:111–23.
[29] Pannirselvam N, Raghunath PN, Suguna K. Neural network for performance of glass fibre reinforced polymer plated RC beams. Am J Eng Appl Sci 2008:183–8.
[30] Perera R, Barchin M, Artega A, De Diego A. Prediction of the ultimate strength of reinforced concrete beams FRP-strengthened in shear using neural networks. Compos Part B Eng 2010;41:287–98.
[31] Razaqpur AG, Isgor BO, Greenaway S, Selley A. Concrete contribution to the shear resistance of fiber reinforced polymer reinforced concrete members. J Compos Constr, ASCE 2004;8(5):452–60.
[32] Razaqpur AG, Isgor OB. Proposed shear design method for FRP reinforced concrete members without stirrups. ACI Struct J 2006;103(1):93–102.
[33] Razaqpur AG, Spadea S. Resistenza a taglio di elementi di calcestruzzzo reinforzatti es taffe di FRP. In: Proc of AIAS 2010, 39th national congress of Italian association of stress analysis, Calabria, Italy; 2010.
[34] Swamy N, Aburawi M. Structural implications of using GFRP bars as concrete reinforcement. In: Proceedings of the third international symposium on non-metallic (FRP) reinforcement for concrete structures (FRPRCS-3), vol. 2. Sapporo (Japan): Japan Concrete Institute; 1997. p. 503–10.
[35] Tariq M, Newhook JP. Shear testing of FRP reinforced Concrete without transverse reinforcement. In: Proceedings of CSCE 2003-anuual conference, Moncton, NB, Canada; 2003. p. 10.
[36] Tottori S, Wakui H. Shear capacity of RC and PC beams using FRP reinforcement. In: Fiber-reinforced-plastic reinforcement for concrete structures, SP-138. Detroit: American Concrete Institute; 1993. p. 615–32.
[37] Tureyen AK, Frosch RJ. Shear tests of FRP-reinforced concrete beams without stirrups. ACI Struct J 2002;99(4):427–34.
[38] Tureyen AK, Frosch RJ. Concrete shear strength: another perspective. ACI Struct J 2003;100(5):609–15.
[39] Weigan FM, Abdalla HA. Shear capacity of concrete beams reinforced with fiber reinforced polymers. Compos Struct 2005;71(1):130–8.
[40] Yang KH, Ashour AF, Song JK, Lee ET. Neural network modelling for shear strength of reinforced concrete deep beams. Struct Build 2008;161(1):29–39.
[41] Yost JR, Gross SP, Dinehart DW. Shear strength of normal strength concrete beams reinforced with deformed GFRP bars. J Compos Constr, ASCE 2001;5(4):263–75.
[42] Zhao W, Mayama K, Suzuki H. Shear behaviour of concrete beams reinforced by FRP rods as longitudinal and shear reinforcement. In: Proceedings of the second international RILEM symposium on non-metallic (FRP) reinforcement for concrete structures (FRPRCS-2), Ghent, Belgium; 1995. p. 352–59.